Article │ Received 5 February 2026; Revised 26 May 2026; Accepted 28 May 2026; Published 16 June 2026
https://doi.org/10.55092/sc20260010

Statistical evaluation of cementitious composites containing rice husk ash and recycled steel fibers

Kaushal Kumar[1], Prawar Chaudhary[2], Anil Dhanda[3], Preeti Rustagi[4], Roopsi Rathee[5], Rishabh Arora[6], Karan Gehlot[7], Ashhad Imam[8,*] and Nishant Yadav[9]

[1] Department of Mechanical Engineering, K.R. Mangalam University, Gurugram, India
[2] Department of Mathematics, School of Basic and Applied Sciences, K.R. Mangalam University, Gurugram, India
[3] Department of Mathematics, Asian School of Business, Asian Education Group, Noida, India
[4] Faculty of Commerce and Management, SGT University, Gurugram, India
[5] Department of Computer Science and Application, IIMT College of Engineering, Greater Noida, India
[6] Department of Civil Engineering, Amity University, Gurugram, India
[7] Amity Institute of Applied Sciences, Amity University, Noida, India
[8] Department of Civil Engineering, Sam Higginbottom University of Agriculture Technology and Sciences, Prayagraj, India
[9] Department of Civil Engineering, Guru Ghasidas Vishwavidyalaya, Bilaspur, India

* Correspondence author; E-mail: ashhad.imam@shiats.edu.in.

Highlights:

- A Central Composite Rotatable Design (CCRD)—based RSM framework was employed to statistically evaluate the combined effects of rice husk ash content, recycled steel fiber aspect ratio, and water–cement ratio on concrete performance.
- Analysis of Variance (ANOVA) results reveal that compressive strength, flexural strength, and water absorption are governed primarily by interaction effects among mixture parameters rather than isolated variable contributions.
- The study delivers experimentally supported, trend-level insights into RHA- and recycled steel fiber–modified cementitious composites, supporting their controlled application in structural engineering contexts.

Abstract: This study presents a statistical evaluation of cementitious composites incorporating rice husk ash (RHA) and recycled steel fibers using a structured experimental design. A Central Composite Rotatable Design (CCRD) within the framework of Response Surface Methodology (RSM) was employed to examine the combined influence of RHA content, recycled steel fiber aspect ratio, and water–cement ratio on selected properties of concrete. A total of twenty experimental mixes were prepared according to the design matrix, and compressive strength, flexural strength, and water absorption were measured as response variables. Material characterization was limited to X-ray

fluorescence–based oxide composition for cement and RHA and scanning electron microscopy–energy dispersive spectroscopy (SEM–EDS) based morphological documentation for RHA. The experimental results were analyzed using analysis of variance to identify statistically supported trends and interaction effects within the investigated parameter ranges. The findings indicate that strength-related responses and water absorption are governed primarily by interaction effects among mixture parameters rather than by individual variables acting independently. The results are interpreted within the investigated design space (10%–20% RHA replacement), and no comparison with control mixtures (0% RHA) is implied. This study provides statistically supported, trend-level insights into the behavior of RHA- and recycled steel fiber–modified cementitious composites under the defined experimental conditions. The results contribute experimental and statistical evidence relevant to structural engineering applications where controlled modification of concrete mixtures is of interest.

Keywords: cementitious composites; structural concrete; rice husk ash; recycled steel fibers; response surface methodology; sustainability; circular economy

1. Introduction

The construction industry is faced with a challenge today: it has to meet the growing need for infrastructure while keeping the environmental impact low. Rapid urbanization, increased population, and increasing standards of living have caused concrete, one of the most popular building materials, to be in greater demand across the world [1,2] is Ordinary Portland cement (OPC), the primary ingredient in concrete, accounts for almost 8% of the world's CO_2 emissions [3,4]. Its production consumes non-renewable resources and is damaging to the environment. At the same time, the management of industrial and agricultural wastes is a major problem [5]. By products like the ash from coal combustion in thermal power stations [6,7], the ash of rice husk (RHA) from rice milling [8,9], and the recycled steel fiber from waste tires, might offer beneficial solutions to the sustainable reuse problem [10–12]. RHA, which accounts for approximately 20%–25% of the total rice husk mass in the world, is high in amorphous silica and has high pozzolanic activity. When added at proper levels it can help refine the microstructure of concrete, making the matrix of concrete denser, durable and less permeable. However, its performance is very much dependent upon the way it is processed, the fineness in which it is ground, and the ratio to which it replaces cement. Recycled steel fibers also enhance the mechanical performance by bridging cracks, energy absorption and post cracking resistance, particularly when the length/diameter ratio (aspect ratio) of recycled steel fibers is ranged from 60 to 140 [13–16]. They also benefit the environment by keeping the tires out of landfills. Although RHA and steel fiber each have certain advantages, most studies have been simple, single-factors experiments. This restricts the knowledge of the interaction of RHA content, aspect ratio of fiber and water-cement ratio. Numerous studies are available regarding the waste utilization as the sustainable cementitious materials [17–19]. Utilizing industrial, agricultural, and general waste as Supplementary Cementitious Materials (SCMs) or alternative binders is a critical strategy to reduce carbon footprints, manage landfill waste, and enhance concrete durability [20–22]. However rare or very few studies employ a systematic and statistically driven approach like the Response Surface Methodology (RSM) to determine linear, quadratic and interaction effects with fewer tests [23,24]. Therefore, there is a need to study the combined effect of these variables on compressive

strength, flexural strength and water absorption so that we can build a high performance, sustainable and durable cementitious material.

The present work is aimed to fill this gap by using RSM to assess the individual and interaction effects and identify statistically supported trends, and a set of parameters that provide a balance between the mechanical performance and permeability. This study is focused on the simultaneous, multivariate optimization of RHA and recycled steel fibers in order to capture the synergistic effects that other studies often do not, and provide a data driven framework for creating sustainable and high performance cementitious composites.

2. Materials and methods

2.1. Characterization and morphological analysis of materials

The materials used for this study were studied to demonstrate their chemical composition and shape before mixing. RHA and OPC were analyzed using x ray fluorescence (XRF) to determine the oxide contents. The XRF results for RHA and OPC are presented in Figure 1a,b and give details of the quantities of each of the main oxides contained in each material. The XRF test only informs us of the chemical composition it does not identify mineral types or distinguish crystalline from amorphous parts.

The shape and structure of ash of rice husk were investigated by scanning electron microscopy (SEM) combined with energy dispersive spectroscopy (EDS). We used a ZEISS scanner with EDS detector. Figure 2 gives some indication of the appearance of the SEM images and the EDS spectra, which show the surface appearance and the elements present at the selected magnifications. This study was limited to visual and elemental documentation; no quantitative microstructural and phase analysis was conducted.

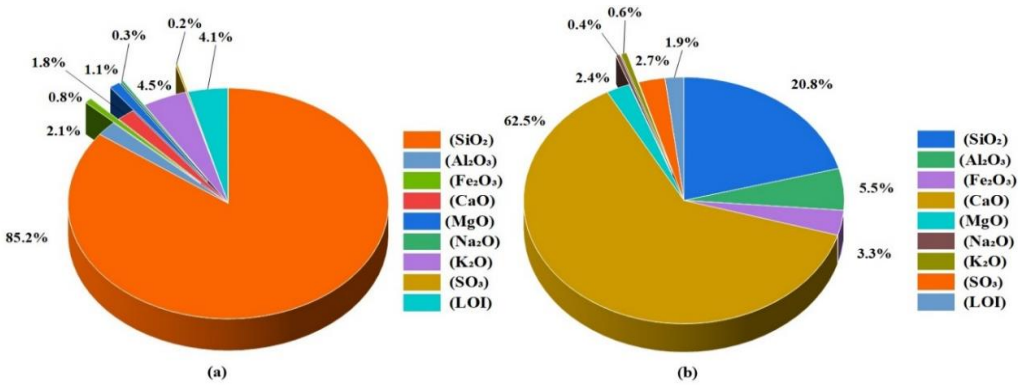

Figure 1. XRF results—oxide composition of **(a)** RHA and **(b)** OPC.

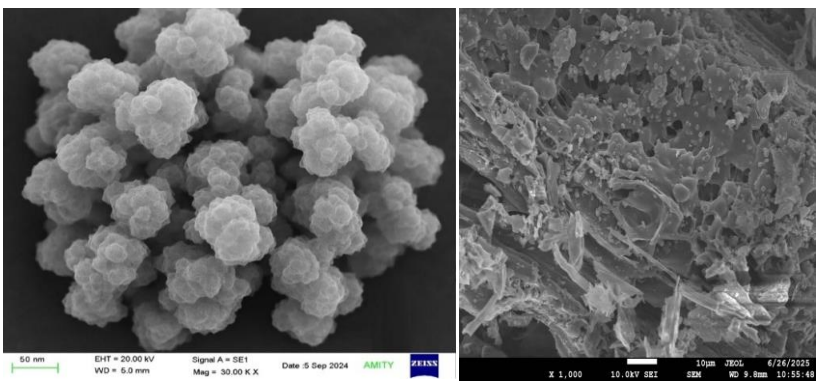

Figure 2. SEM EDS and surface roughness of rice husk ash.

2.2. Experimental setup and range of parameters

We have employed a CCRD, RSM in order to study the effect of amount of RHA, shape of recycled steel fibers and water-cement ratio on concrete. Twenty different mixes were made according to CCRD which includes main levels, extreme levels and middle levels. The ranges selected were: steel fiber aspect ratio ranging from 60 to 140, water-cement ratio between 0.30 and 0.40 and RHA content between 10 percent and 20 percent of the cement weight.

For each test, we first dry mix cement, RHA, fine aggregate and coarse aggregate in order to spread evenly. Then we slowly added the recycled steel fiber to prevent them from sticking to each other, and then the water and water reducing admixture were added according to the design needs. The fresh concrete was mixed until it was smooth and uniform then poured into standard molds and left to cure. All mixes were made the same way so that the test results could be compared reliably.

The high proportion of silica ($SiO_2 \approx 85.2\%$) and relatively low CaO content indicate the potential suitability of RHA as a supplementary cementitious material; however, direct verification of pozzolanic reactivity would require additional mineralogical and surface characterization (Figure 1).

3. Experimental design and optimization framework

3.1. Design of experiment

We used grade 43 OPC that follows IS 8112 as the main binder. All the cement was from the same batch to ensure consistency in the experiment. Its specific gravity is 3.15. RHA was used partially to replace the cement. RHA was from burning rice husks at a local waste plant. After burning, we ground and worked it through a sieve to get rid of the big pieces. Its specific gravity is 2.28. We determined the chemical composition of OPC and RHA by XRF. The results can be seen in Figure 1a for RHA and Figure 1b for OPC. We only reported oxide composition, and we did not separate crystalline and amorphous.

The reinforcement was recycled steel fibers. The fibers were extracted from the used vehicle tires and mechanically separated and cleaned by hand. They are about 0.25 mm in diameter. So, we took cuts to get aspect ratios of 60, 100 and 140. Their specific gravity is about 5.0 and they can take about 700 N/mm^2 of tension. Steel fibers composed 1% of the total volume in all mixes. We used river sand of Zone II grading (IS 383) fine aggregate. Its specific gravity is 2.58. Crushed granite of 10–20 mm size (*i.e.* coarse aggregate) Specific gravity of crushed granite is 2.70. Both aggregates used when the surfaces of the aggregates were just dry after being fully saturated. We used pure drinking water which is according to IS 456 for mixing and curing. We included a commercial high-range water reducer, to the extent of about 1.5 per cent of the binder weight, to make all mixes workable.

The experimental design adopted in this study follows a CCRD within the framework of Response Surface Methodology. While Table 1 presents the coded factorial levels (−1, 0, +1) for clarity, the complete design matrix includes factorial points, axial (star) points at $\pm \alpha$ levels, and replicated center points. For three independent variables, the CCRD structure ensures rotatability and enables reliable estimation of linear, interaction, and quadratic effects within the selected design space. A total of 20 experimental runs were generated using Minitab software, comprising 8 factorial points, 6 axial points, and 6 center points. The axial points extend beyond the factorial levels to capture curvature effects, thereby enhancing the predictive capability of the developed response surface models. This design

strategy ensures efficient exploration of the parameter space while maintaining statistical robustness with a limited number of experiments. Using Minitab statistical software, a total of 20 experimental runs were generated according to the CCRD framework. This allowed for the exploration of both linear and nonlinear interactions between the variables and their collective influence on the target responses: compressive strength, flexural strength, and water absorption. The value of α was selected based on standard rotatability conditions for three factors. The full experimental design matrix and corresponding mix proportions are presented in subsequent sections.

Table 1. Independent variables and their experimental levels.

Factor	Code	Unit	−α (Axial)	−1 (Low)	0 (Center)	+1 (High)	+α (Axial)
Aspect Ratio (Steel Fiber)	A	—	40	60	100	140	160
Water–Cement Ratio	B	—	0.28	0.30	0.35	0.40	0.42
RHA Content	C	%	8	10	15	20	22

3.2. Detailed mix design and testing procedure

All 20 experimental batches of concrete mix proportions were developed according to the CCRD [25,26]. The parameters taken are the aspect ratio of steel fibers (A), the water-cement ratio (B), and the RHA content (C). The volume proportion of steel fiber was fixed at 1%, and the dosage of superplasticizer was adjusted to ensure similar workability of all mixes. The detailed mix proportions used for all experimental batches are summarized in Table 2 below.

Table 2. Detailed mix proportions of cementitious composites.

Component	Unit	Quantity
Cement (OPC)	kg/m ^{3}	315–360*
Rice Husk Ash (RHA)	kg/m ^{3}	35–90*
Fine Aggregate (Sand)	kg/m ^{3}	650
Coarse Aggregate (10–20 mm)	kg/m ^{3}	1200
Water	kg/m ^{3}	105–144*
Steel Fibers (1% volume fraction)	kg/m ^{3}	~78
Superplasticizer	% (by binder weight)	1.40–1.65

To find out the experimental evaluation of the concrete mixtures with RHA and recycled steel fibers, a rigorous testing program was followed, which followed the standardized procedures provided by the Bureau of Indian Standards (BIS). The aim was to determine important mechanical and durability parameters, and that they would be consistent, accurate, and reproducible among the 20 mix combinations. Compressive strength was determined using standard concrete cubes of size 150 mm × 150 mm × 150 mm, tested using a calibrated compression testing machine (Make: Aimil CTM IS: 14858 (2000) with an accuracy of ± 1. The workability of fresh concrete was assessed through the slump test, as per IS 1199 (Part 2): 2018, and the slump was recorded in millimeters. Water absorption was evaluated to assess capillary moisture uptake characteristics and pore structure development by immersing cylindrical specimens (100 mm diameter × 200 mm height) in water for 24 hours, following the guidelines of IS 2386 (Part 3):1963. Flexural strength was tested using prismatic beams of dimensions 100 mm × 100

mm × 500 mm under a two-point loading arrangement, with calibrated machines (Make: Aimil FTM, IS 516 BS1881, with an accuracy of ± 1%). The average of three tests has been calculated for the average compression strength, average flexural strength, and water absorption. The final value of all the results has been tabulated in Table 3. These standardized test procedures ensured a comprehensive and credible characterization of both fresh and hardened properties of the fiber-reinforced, RHA-blended concrete. The results served as the foundation for modeling, analysis, and optimization using Response Surface Methodology.

Table 3. Experimental result as per the inputs.

Mix No.	Aspect Ratio	W/C Ratio	RHA (%)	Superplasticizer (%)	Slump (mm)	Compressive Strength (MPa)	Flexural Strength (MPa)	Water Absorption (%)
E01	60	0.40	20	1.60	78	27.57	5.85	5.66
E02	100	0.35	15	1.50	82	38.70	6.65	4.98
E03	100	0.30	10	1.40	76	35.73	6.55	5.55
E04	140	0.35	10	1.50	80	36.97	6.80	5.54
E05	60	0.30	10	1.40	75	36.00	6.15	5.48
E06	100	0.30	20	1.55	74	37.15	6.55	5.40
E07	100	0.40	15	1.60	84	36.61	6.50	5.17
E08	100	0.40	20	1.65	83	32.33	6.25	5.60
E09	100	0.35	10	1.45	81	34.10	6.40	5.42
E10	140	0.40	10	1.60	82	35.64	6.65	5.76
E11	60	0.30	15	1.45	77	39.06	6.40	4.94
E12	60	0.35	15	1.50	80	35.57	6.25	4.96
E13	60	0.35	20	1.55	79	32.46	6.00	5.65
E14	60	0.30	20	1.55	74	35.89	6.15	5.26
E15	100	0.40	10	1.60	83	29.89	6.25	5.50
E16	140	0.35	15	1.55	81	41.21	7.05	5.03
E17	60	0.35	10	1.45	79	33.90	6.00	5.32
E18	140	0.40	15	1.60	84	39.18	6.90	5.10
E19	140	0.35	20	1.55	80	37.57	6.80	5.57
E20	140	0.30	10	1.45	76	42.31	6.95	5.51

The superplasticizer dosage was adjusted within a narrow range (1.40%–1.65% by weight of binder) to maintain consistent workability across all mixes. The slump values were controlled within a range of approximately 74–84 mm, ensuring comparable fresh concrete behavior and minimizing the influence of workability variations on mechanical properties.

4. Results and discussion

The experimental results obtained by the RSM are analyzed, with the focus of the analysis on finding main trends and interactions between variables. Since some of the regressions models are only moderately significant, the relative performance of each factor rather than suggesting exact predictions has been investigated. In this section the design importance of statistically significant and nearly significant factors has been studied.

4.1. Compressive strength analysis

The compressive strength of the cementitious composites with RHA and recycled steel fibers showed a significant change throughout the experimental spectrum of the CCRD. Table 4 analysis of variance shows that the overall regression model is not significant at the 95% level ($p = 0.092$), which indicates that compressive strength does not depend on one particular dominant factor. Nevertheless, a number of individual and interaction effects exhibit statistically significant trends, which suggests that the mechanical response is largely controlled by compound parameter interactions other than individual effects. Such behavior may also be explained by the microstructural changes and enhancements of the interfacial transition zone (ITZ), which is also addressed in Section 4.5. One of the linear effects is the aspect ratio of recycled steel fibers, which has a statistically significant effect on compressive strength ($p = 0.046$). An increase in aspect ratio fibers increases the efficiency of crack-bridging, internal confinement, and allows the more efficient redistribution of stress in the matrix during compressive loading. These processes slow down the microcrack propagation and help in enhanced load-bearing capacity. The same has been observed in recent research where high fiber aspect ratio was observed to increase compressive resistance by increasing matrix continuity and crack arresting behavior [27].

Table 4. Analysis of variance for compressive strength.

Source	DF	Adj SS	Adj MS	F-value	p-value
Model	9	42.42	4.71	2.43	0.092
Linear	3	19.32	6.44	3.32	0.065
├ A: Aspect ratio	1	10.09	10.09	5.19	**0.046**
├ B: W/C ratio	1	1.23	1.23	0.64	0.444
├ C: RHA content	1	8.00	8.00	4.12	0.070
Square	3	7.78	2.59	1.34	0.317
Interaction	3	15.32	5.11	2.63	0.108
├ B × C	1	14.58	14.58	7.51	**0.021**
Error	10	19.42	1.94	—	—
Lack of fit	5	11.15	2.23	1.35	0.376
Total	19	61.85	—	—	—

The correlation between water-cement ratio and RHA content is significant ($p = 0.021$), which suggests that the compressive strength is also highly affected by the effects of hydration states and pozzolanic activity in combination. A moderate usage of RHA helps a secondary hydration by creating more calcium silicate hydrate (C-S-H) gel which optimizes the pore structure and increases densification of the matrix. Nevertheless, this advantage is very much reliant on the presence of enough water to support primary and secondary hydration reactions. Past research attests that RHA-blended system works best with optimality of water-cement ratios, and excess water results in higher porosity and dilution of hydration products [28,29]. This type of interaction-based behavior also contributes to why the effect of RHA only has a near-significant effect ($p = 0.070$), since its effect is inherently connected to the state of hydration.

Response surface and contour plots (Figures 3 and 4) show that the compressive strength is maximized at water cement ratio of about 0.35, RHA content within a range of 10%–15%, and at high aspect ratios of fibers. In this optimum area, there is a balance of density of the matrix, the reinforcement of fiber, as well as the efficiency of hydration.

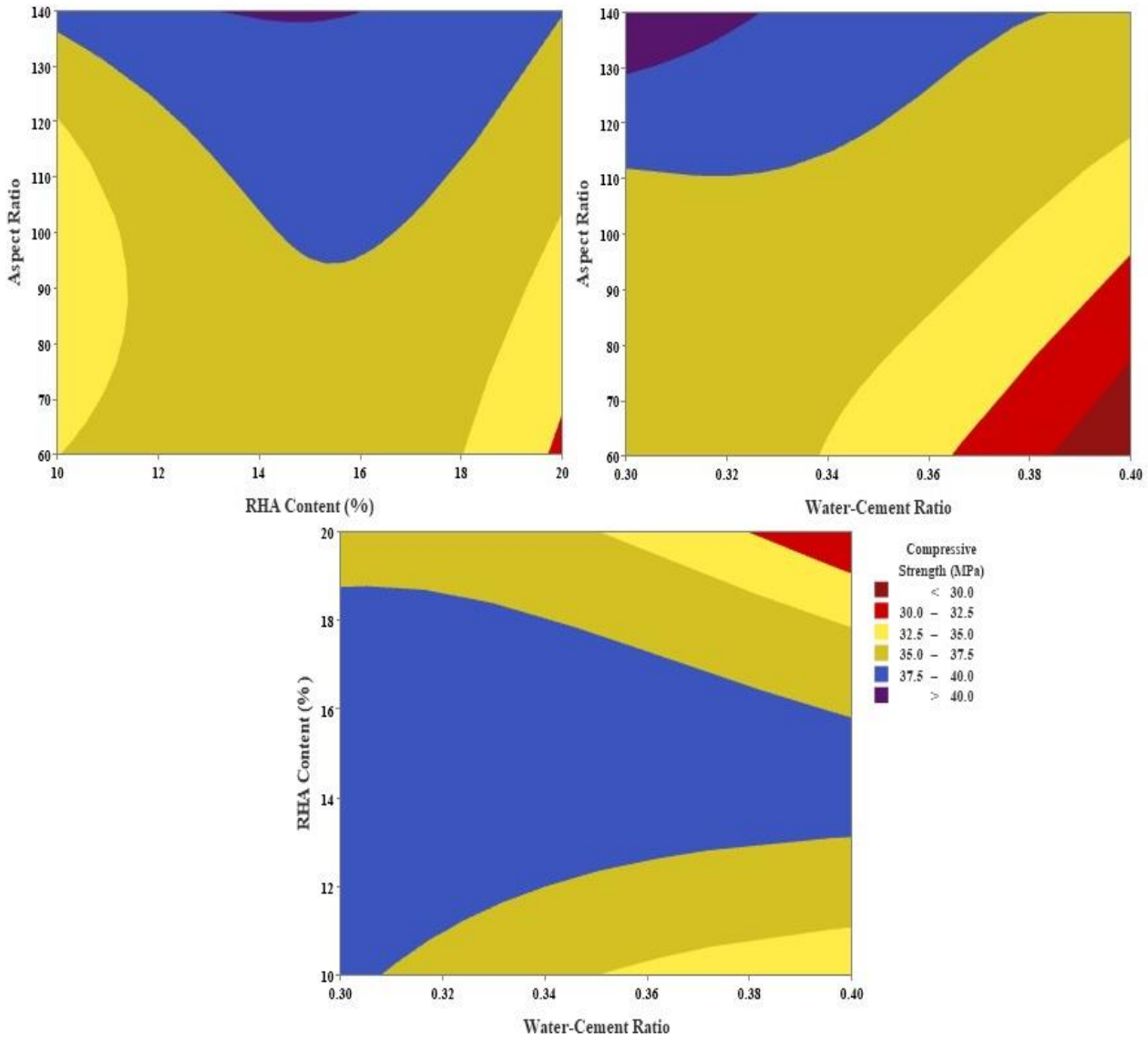

Figure 3. Contour plots for the compressive strength.

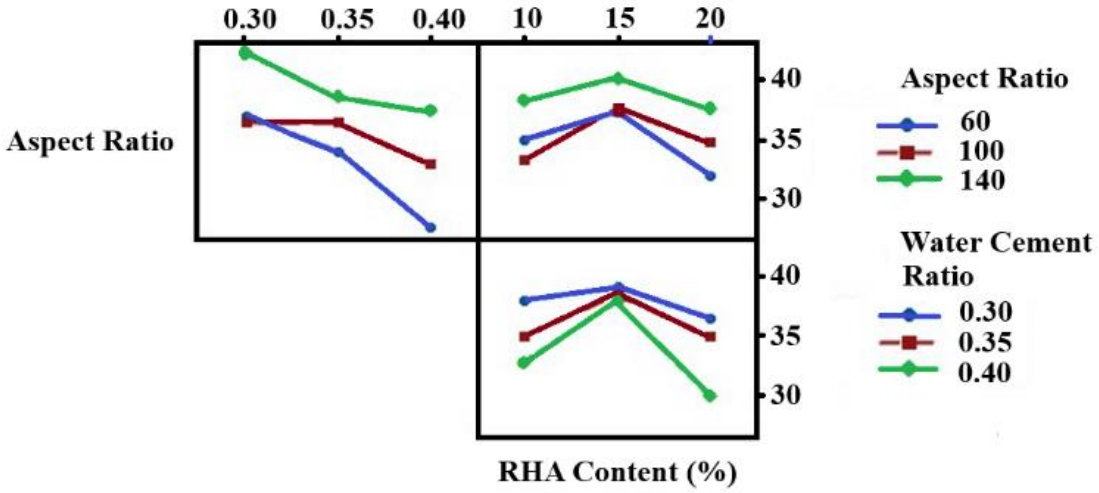

Figure 4. Interaction between different response factors for compressive strength.

At this optimum range, there is a systematic decrease in compressive strength. This decline can be attributed to three mechanisms that are interconnected, hydration kinetics, reactive material balance, and phase composition evolution. To begin with, too much cement substitution with RHA lowers the ratio of clinker, thus restricting the supply of alite and belite phases that cause early hydration and primary C-S-H development. This causes reduced rate of hydration and low initial strength development. Second, despite the fact that RHA supplies reactive amorphous silica, its pozzolanic activity requires adequate calcium hydroxide produced in the course of cement hydration. The lower cement fraction at higher replacement levels might not be able to provide sufficient $Ca(OH)_2$ to maintain a successful secondary hydration hence the absence of full clinker dilution compensation. Third, regarding phase composition, too much RHA moves the system to lower levels of portlandite and lower total amount of hydration products. In case the reactivity or fineness of RHA is not high enough, it can result in a less continuous binder matrix and high porosity. Besides, an increase in the RHA content may lead to more water demand, which impacts the workability and hydration efficiency. The cumulative effect of these is the eventual decrease in compressive strength after the optimum replacement level. The findings have shown that compressive strength in RHA-steel fiber composites is dictated by the complex interaction of hydration processes, microstructural development, and fiber-matrix interaction, which supports the need to optimize multi-parameters within a specified design space.

Although the developed regression model for compressive strength did not satisfy the overall significance criterion at the 95% confidence level, the response surface analysis was retained to examine interaction-oriented response trends within the investigated experimental domain. The generated surface plots should therefore be interpreted as exploratory statistical representations of the coupled effects of RHA content, recycled steel fiber aspect ratio, and water–cement ratio, rather than as highly predictive optimization models. Consequently, the observed parameter combinations associated with improved compressive strength are discussed as favorable trends within the investigated design space rather than definitive optimum conditions.

4.2. Flexural strength analysis

Flexural strength values of CCRD experiments remained in a close range, which demonstrated the bending performance depends not on a single cause, but has several interacting factors. The overall regression model for flexural strength showed in Table 5 is not statistically significant ($p = 0.170$). This means that higher order terms and individual linear effects are not completely able to explain flexural behavior in the design space studied. The observed behavior is further supported by ITZ refinement and enhanced fiber–matrix bonding mechanisms discussed in Section 4.5.

Although the global model is not significant, water-cement ratio and RHA content interaction is significant ($p = 0.038$). This demonstrates that the performance with respect to bending is determined primarily by the joint action of these two factors. The interaction is a representation of how continuity of the matrix and the quality of interface is dependent on the amount of hydration products and the pozzolanic reaction. The introduction of a moderate amount of RHA leads to an improvement of microstructure by secondary C-S-H formation whereas an optimized water-cement ratio provides the appropriate workability and fibre distribution. Both are important to resist the tensile stresses during bending.

The near significant ($p = 0.066$) linear effect of RHA content suggests that it aids in improving interfacial bonding, and reduce the onset of microcracks. A better pore structure and improved paste

quality transfers stress better across the matrix-fiber interface, which increases the resistance to flexural cracking. Even though the aspect ratio of steel fibre is not a statistically significant factor, it still has an effect on the bending response through its interactions with the matrix composition and workability. Fibers having higher aspect ratio provide better bridging capability of cracks and transfer of load after cracking, provided that the matrix remains coherent and the fibers remain dispersed.

Response surface plots (Figures 5 and 6) indicate that the optimum flexural strength results from a balanced combination of moderate RHA replacement, controlled water-cement ratio and relatively high fiber aspect ratios. These results reinforce that bending behavior in fiber reinforced, pozzolan modified cementitious composites are governed by cooperative mechanisms, *i.e.* matrix refinement, fiber matrix interaction and crack bridging efficiency, and not by any single material component.

Table 5. Analysis of variance for flexural strength.

Source	DF	Adj SS	Adj MS	F-value	p-value
Model	9	2.30	0.256	1.88	0.170
Linear	3	1.02	0.339	2.49	0.120
├ A: Aspect ratio	1	0.288	0.288	2.11	0.177
├ B: W/C ratio	1	0.151	0.151	1.11	0.317
├ C: RHA content	1	0.580	0.580	4.26	0.066
Interaction	3	0.844	0.281	2.07	0.168
├ B × C	1	0.781	0.781	5.74	**0.038**
Error	10	1.36	0.136	—	—
Lack of fit	5	0.988	0.198	2.65	0.155
Total	19	3.66	—	—	—

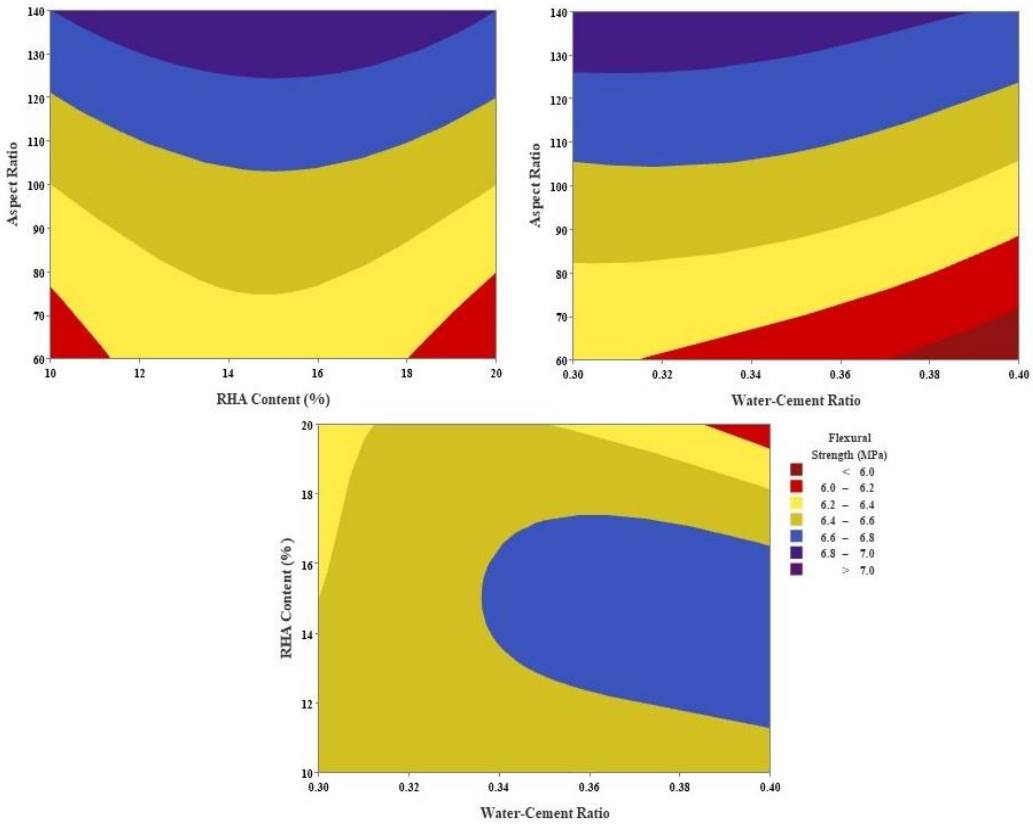

Figure 5. Contour plots for flexural strength.

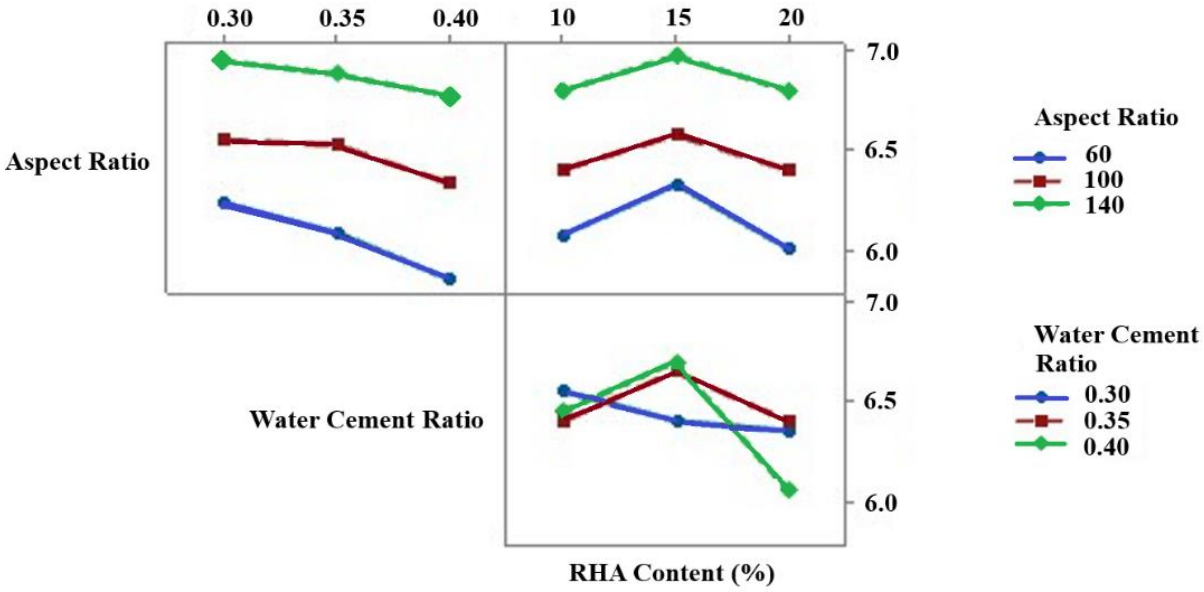

Figure 6. Interaction between different response factors for flexural strength.

Similar to the compressive strength model, the overall regression model for flexural strength exhibited moderate statistical significance and should therefore be interpreted with caution. The RSM analysis in the present study was primarily intended to identify interaction behavior and relative response tendencies among the investigated variables rather than to establish universally predictive optimization equations. Accordingly, the response surfaces are discussed in terms of trend-level insights and favorable experimental combinations within the investigated parameter range.

It is important to note that the developed regression models were used primarily for exploratory interpretation of response interactions within the CCRD framework. Although certain response models did not achieve strong overall statistical significance at the 95% confidence level, the analysis still provided useful qualitative insight into the coupled influence of mixture parameters. Therefore, the findings derived from the response surface analysis should be interpreted as indicative trends within the investigated experimental region rather than definitive predictive relationships.

4.3. Water absorption analysis

Water absorption was employed in this study as a rapid test to determine to what extent the material allows water through. It provided better patterns in the data than the strength test. Table 6 shows that the straight-line part of our math model is important ($p = 0.046$), that is to say that first order effects are mostly in control of water absorption in the ranges we looked at. However, the overall model is not statistically strong ($p = 0.154$), that is, the higher order and interaction terms do not provide much value.

Among all the factors we tested, RHA content is the biggest factor affecting water absorption ($p = 0.047$). This occurs because RHA has a reaction with mix and it has small particles making the pores smaller and the matrix more dense when used at moderate level. The additional Calcium Silicate Hydrate (C-S-H) gel makes it difficult for the water to pass through, which slows down absorption [30]. But too much RHA, can increase the requirement of water and result in incomplete hydration which could negate the benefits.

The water-cement ratio also alters the absorption. Higher ratios indicate increased uptake of water due to the formation of more pores. This is a link between water-cement ratio, pore structure and permeability that is known. Steel fiber aspect ratio is smaller effect. Steel fibers don't block pores directly but they help in keeping the mix together and control the tiny cracks rather than changing the pore structure.

Contour plots (Figures 7 and 8) indicate that the minimum amount of water absorption occurs when RHA is around 10–15 percent and water-cement ratio is low to moderate. The fact that interaction effects are not statistically significant serves as proof of absorption of water by primarily linear parameter affects in our design. Since we only studied short term absorption, the results only point to trends in permeability, not complete long-term durability. Still, the results demonstrate the use of the right amount of RHA that reduces water absorption and makes the cement mix more water resistant.

Table 6. Analysis of variance (ANOVA) for water absorption.

Source	DF	Adj SS	Adj MS	F-value	p-value
Model	9	1.71	0.190	1.96	0.154
Linear	3	1.12	0.372	3.83	**0.046**
├ A: Aspect ratio	1	0.369	0.369	3.80	0.080
├ B: W/C ratio	1	0.247	0.247	2.54	0.142
├ C: RHA content	1	0.500	0.500	5.15	**0.047**
Interaction	3	0.344	0.115	1.18	0.366
Error	10	0.971	0.097	—	—
Lack of fit	5	0.676	0.135	2.29	0.192
Total	19	2.69	—	—	—

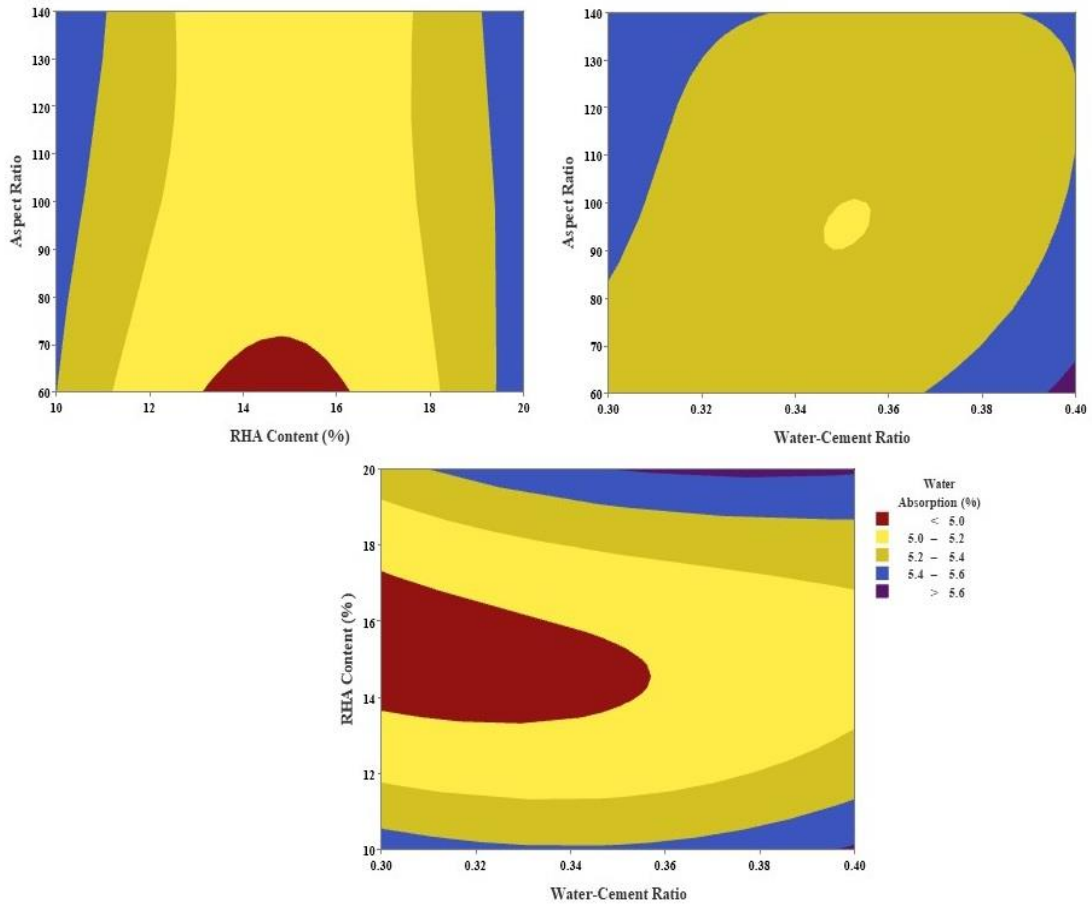

Figure 7. Contour plots for water absorption.

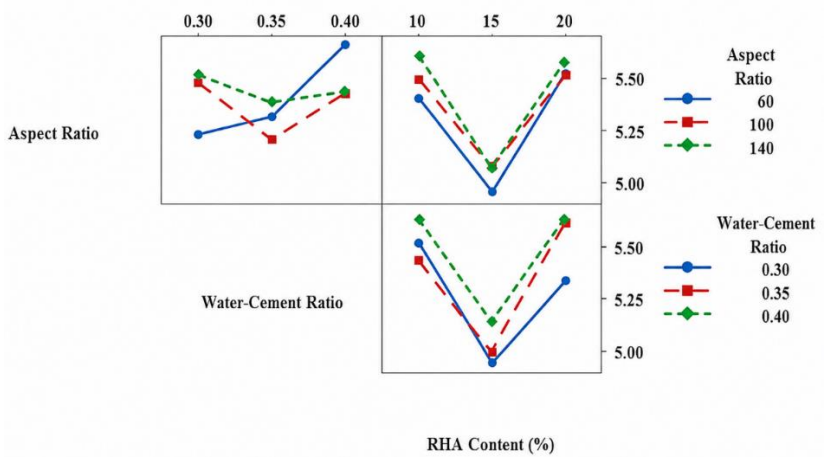

Figure 8. Interaction between different response factors for water absorption.

It should be noted that the water absorption test employed in the present study reflects short-term capillary moisture uptake behavior under immersion conditions and should not be interpreted as a direct measure of long-term permeability or impermeability performance. Therefore, the observed reductions in water absorption are discussed only in the context of capillary absorption-related behavior within the investigated experimental framework.

4.4. Analysis of parameters through response surface methodology

RSM has been employed to investigate the assistance of quantity of RHA and aspect ratio of steel fibers in connection to compressive strength as shown in Figure 9. The results indicate a clear interaction, *i.e.* that the strength is dependent on both parts and on the way they work together.

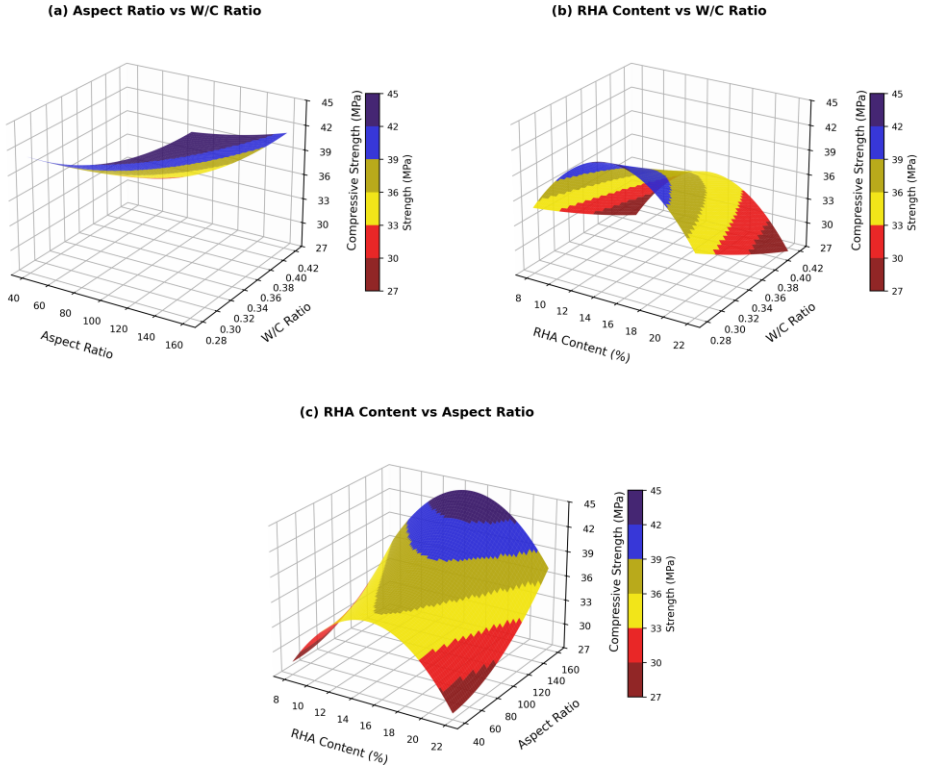

Figure 9. RSM surface plots for compressive strength: **(a)** aspect ratio *vs.* water–cement ratio; **(b)** RHA content *vs.* water–cement ratio; and **(c)** RHA content *vs.* aspect ratio.

Using 10%–15% RHA produces the best compressive strength particularly if the aspect ratio of steel fibers has an aspect ratio of 80–100. This is because RHA reacts with the mix to form increased C-S-H gel and also closes the pore structure of the mix making the cement matrix denser. Steel fibers with moderate-to-high aspect ratio also help to bridge cracks and transfer stress to improve performance.

If the RHA exceeds the optimum, the strength reduces because the cement mix is diluted and more water is required. High aspect ratios can also cause fibers to bunch together and to cause weak spots. The response surface provides that the best strength is only achieved when the RHA content and fiber geometry are in balance, demonstrating the usefulness of RSM for optimization of many parameters in cementitious composites.

4.5. Microstructural mechanism and ITZ evolution

The enhancement in the mechanical performance observed in the present study may be associated with the combined influence of secondary pozzolanic reactions, pore structure refinement, and possible modification of the interfacial transition zone (ITZ). RHA, owing to its high amorphous silica content, can participate in secondary hydration reactions with calcium hydroxide $(Ca(OH)_2)$ generated during cement hydration, potentially contributing to the formation of additional calcium silicate hydrate (C-S-H) gel. Such reactions are commonly reported in the literature to improve matrix densification and reduce pore connectivity in cementitious systems.

In conventional concrete, the ITZ surrounding aggregates and fibers is generally considered a relatively porous and weaker region due to localized accumulation of hydration products and micro voids.

The incorporation of finely divided pozzolanic materials such as RHA may contribute to refinement of this region by improving particle packing and reducing localized porosity. These effects may, in turn, enhance stress transfer between the cement matrix and recycled steel fibers, thereby contributing to improved crack-bridging behavior and resistance to crack propagation.

However, it should be emphasized that the present study did not include direct quantitative microstructural characterization of hardened composites, hydration products, or ITZ morphology. The SEM/EDS investigations performed in this work were limited to qualitative characterization of the raw materials rather than detailed analysis of the hardened cementitious matrix. Therefore, the proposed mechanisms related to C-S-H evolution, ITZ refinement, and fiber–matrix interfacial interactions should be regarded as theoretical interpretations inferred from previously reported literature and the experimentally observed macroscopic trends within the investigated design space.

Previous studies, including molecular dynamics and nanoscale investigations reported in the literature [31–33], have suggested that interfacial interactions, hydration-product distribution, and water-mediated cohesion may influence the mechanical response of cementitious materials. Nevertheless, the present work does not provide direct experimental evidence at the nanoscale to verify such mechanisms. Accordingly, the discussion presented here is intended only to provide possible mechanistic explanations for the statistically observed trends in compressive strength, flexural strength, and water absorption.

Overall, the experimentally observed behavior may reasonably be attributed to the combined effects of matrix densification, secondary hydration reactions, and possible improvement in fiber–matrix interaction within the investigated parameter range. These interpretations should be considered as trend-level insights

rather than definitive microstructural conclusions, particularly in view of the absence of detailed phase analysis or quantitative microstructural investigations in the present study.

It should be noted that the present study did not include SEM examination of fractured composite specimens, fiber pull-out morphology, crack propagation paths, or quantitative characterization of the ITZ. Therefore, the discussion regarding crack-bridging mechanisms, fiber–matrix interaction, and ITZ enhancement is based on experimentally observed macroscopic trends together with interpretations reported in previous literature, rather than on direct microstructural evidence obtained in the current investigation. Future studies involving fracture-surface SEM analysis and quantitative ITZ characterization are recommended to establish stronger mechanistic correlation between the observed statistical responses and the underlying microstructural behavior.

5. Conclusion

This study investigated the combined effects of RHA content, recycled steel fiber aspect ratio, and water–cement ratio on the mechanical performance and water absorption behavior of cementitious composites using a CCRD within a RSM framework. The experimental and statistical analyses were conducted to identify interaction-driven trends within the defined design space rather than to establish universally predictive models. Based on the experimental observations and statistical analysis, the following conclusions are drawn:

- Compressive strength varied noticeably across the design space, with peak values observed at RHA contents of 10%–15%, moderate water–cement ratios (~0.35), and higher fiber aspect ratios. Within this range, compressive strength increased by approximately 8%–15% within the investigated design space.
- Increasing RHA content beyond 15% resulted in a compressive strength reduction of approximately 5%–12%, attributed to cement dilution and reduced availability of primary hydration products.
- The aspect ratio of recycled steel fibers exhibited a statistically significant linear effect on compressive strength ($p = 0.046$), with higher aspect ratios contributing to an estimated 6%–10% increase in compressive strength due to improved crack arrest and stress redistribution.
- The interaction between water–cement ratio and RHA content showed a statistically significant influence on compressive strength ($p = 0.021$), confirming that RHA effectiveness is strongly dependent on adequate hydration conditions rather than acting independently.
- Flexural strength values showed limited absolute variation; however, optimal combinations of moderate RHA content and controlled water–cement ratio resulted in a 7%–12% improvement in flexural strength compared to mixes with higher water content or no pozzolanic replacement.
- The interaction between water–cement ratio and RHA content significantly influenced flexural strength ($p = 0.038$), indicating that flexural performance is governed by coupled matrix refinement and fiber–matrix bonding mechanisms.
- Steel fiber aspect ratio, while not statistically significant as a standalone factor for flexural strength, enhanced post-cracking resistance and contributed indirectly to improved bending performance when combined with optimized matrix composition.
- Water absorption decreased systematically with increasing RHA content up to 10%–15%, with a reduction of approximately 10%–18% compared to other experimental combinations, reflecting effective pore refinement and reduced capillary connectivity.

- Increasing the water–cement ratio led to a 15%–25% increase in water absorption, confirming the dominant role of capillary porosity in short-term permeability behavior.
- Water absorption was primarily governed by linear effects ($p = 0.046$), with RHA content identified as the most influential parameter ($p = 0.047$), while interaction terms were statistically insignificant within the investigated design space.
- The combination of moderate RHA replacement (10%–15%), controlled water–cement ratio, and higher recycled steel fiber aspect ratio resulted in simultaneous enhancement of compressive and flexural strength together with reduced measured water absorption, indicating improved capillary moisture uptake characteristics within the investigated experimental range.
- The response surface models developed in this study provided statistically guided interpretation of interaction trends among RHA content, recycled steel fiber aspect ratio, and water–cement ratio within the investigated experimental domain. However, due to the moderate statistical significance of certain regression models, the obtained response surfaces and associated parameter combinations should be interpreted as exploratory trend-level observations rather than universally optimized predictive models. Further experimental validation with expanded datasets and refined statistical modeling is recommended for stronger predictive generalization.

Data availability statement

All experimental data generated and analyzed during this study are included within the article. No supplementary or additional data were generated in this study.

Declaration of generative AI and AI-assisted technologies

The authors did not use generative AI or AI-assisted technologies in the writing of this manuscript.

Authors' contribution

Conceptualization, K.K., P.C., A.D. and A.I.; methodology, R.R., R.A. and K.G.; software, A.D., P.R., R.R. and K.G.; validation, A.D., R.R. and R.A.; formal analysis, P.C., A.D., P.R. and R.A.; investigation, K.K., P.C., A.D., A.I., P.R., and R.A.; resources, K.K., P.C., A.D. and K.G.; data curation, P.C., A.D., A.I., K.G., P.R. and R.A.; writing—original draft preparation, R.R., A.D., K.G., P.R. and R.A.; writing—review and editing, A.D., P.R., A.I., N.Y. and R.A.; visualization, K.K., P.C., A.D., R.R.. and R.A.; supervision, A.I., N.Y.; project administration, A.I., N.Y. All authors have read and agreed to the published version of the manuscript.

Conflicts of interest

There is no conflict among authors.

References

[1] Haba B, Djellali S, Abdelouahed Y, Boudjelida S, Faleschini F, *et al.* Transforming plastic waste into value: a review of management strategies and innovative applications in sustainable construction. *Polymers* 2025, 17(7):881.

[2] Tul Muntaha S, Keitsch M. A pathway for plastic waste in construction materials. *Sustainable Dev.* 2025, 33(1):19–29.
[3] Hasan K, Islam MT, Ferdaus R, Yahaya FM. Experimental study on environment-friendly concrete production incorporating palm oil clinker and cockle shell powder as cement partial replacement. *Mater. Today Proc.* 2022, 107:254–262.
[4] Karadumpa CS, Pancharathi RK. Study on energy use and carbon emission from manufacturing of OPC and blended cements in India. *Environ. Sci. Pollut. Res. Int.* 2024, 31(4):5364–5383.
[5] Salleh SZ, Awang Kechik A, Yusoff AH, Taib MAA, Mohamad Nor M, *et al.* Recycling food, agricultural, and industrial wastes as pore-forming agents for sustainable porous ceramic production: a review. *J. Clean Prod.* 2021, 306:127264.
[6] Castellano J, Sanz V, Cañas E, Sánchez E. Industry-scalable wall tile composition based on circular economy. *Bol. Soc. Esp. Ceram. Vidr.* 2022, 61(4):374–382.
[7] Kumar K, Singh J, Mishra U, Singh S, Kumar P, *et al.* Potential utilization of grounded bottom ash for sustainable stowing applications. *WSEAS Trans. Environ. Dev.* 2025, 21:254–265.
[8] Mahdi SN, Babu RDV, Hossiney N, Abdullah MMAB. Strength and durability properties of geopolymer paver blocks made with fly ash and brick kiln rice husk ash. *Case Stud. Constr. Mater.* 2022, 16:e00800.
[9] Guo Z, Chen Z, Yang X, Zhang L, Li C, *et al.* The influence of rice husk ash incorporation on the properties of cement-based materials. *Materials* 2025, 18(2):460.
[10] Wang Z, Liang X, Wan S, Cao Z, Weng S, *et al.* Experimental and theoretical investigation on axial tensile behavior of ultra-high performance concrete (UHPC) with recycled steel fibers from waste tires. *Constr. Build. Mater.* 2024, 456:139300.
[11] Zhang P, Wang C, Wu C, Guo Y, Li Y, *et al.* A review on the properties of concrete reinforced with recycled steel fiber from waste tires. *Rev. Adv. Mater. Sci.* 2022, 61(1):276–291.
[12] Al-Kheetan MJ, Jweihan YS, Rabi M, Ghaffar SH. Durability enhancement of concrete with recycled concrete aggregate: the role of Nano-ZnO. *Buildings* 2024, 14(2):353.
[13] Anupam BR, Thakur MK, Debbarma S. Synergistic effects of manufactured and recycled steel fibers in paving concrete mixtures. *J. Mater. Civ. Eng.* 2026, 38(2):04025550.
[14] Zhang M, Jing J, Zhang S. Effect of steel fiber content on fatigue performance of high-strength concrete beams. *Sci. Rep.* 2025, 15(1):11815.
[15] Albayati AH, Mohammed AM, Al-Kheetan MJ, Al-ani AF, Oukaili NK, *et al.* Performance enhancement of natural asphalt using waste-derived modifiers: sugarcane molasses and waste engine oil. *Cleaner Waste Syst.* 2025, 11:100261.
[16] Gómez-Cano D, Arias-Jaramillo YP, Beraal-Conea R, Tobón JI. Effect of enhancement treatments applied to recycled concrete aggregates on concrete durability: a review. *Mater. Constr.* 2023, 73(349):e308.
[17] Alsharari F. Utilization of industrial, agricultural, and construction waste in cementitious composites: a comprehensive review of their impact on concrete properties and sustainable construction practices. *Mater. Today Sustainability* 2025, 29:101080.
[18] Wang Y, Huang X, Zhang S, Ma W, Li J. Utilization of ultrafine solid waste in the sustainable cementitious material for enhanced performance. *Constr. Build. Mater.* 2024, 417:135239.

[19] Sakir S, Raman SN, Safiuddin M, Amrul Kaish ABM, Mutalib AA. Utilization of by-products and wastes as supplementary cementitious materials in structural mortar for sustainable construction. *Sustainability* 2020, 12(9):3888.

[20] Oyejobi DO, Firoozi AA, Fernández DB, Avudaiappan S. Integrating circular economy principles into concrete technology: enhancing sustainability through industrial waste utilization. *Results Eng.* 2024, 24:102846.

[21] Ul Haq MZ, Singh S, Vora T, Singh P, Dasarathy AK, *et al.* Low-permeability bentonite–ash–cement composites: optimization using Taguchi design, machine learning, and microstructural characterization. *Eur. J. Mater.* 2025, 5(1):2552664.

[22] Suresh B, Rajkumar PRK. A review on the properties of concrete blended with supplementary cementitious materials from industrial wastes. *AIP Conf. Proc.* 2024, 3187(1):030011.

[23] Montazeri P, Bamshad O, Aghililotf M, Singh P. Mechanical and durability-based life cycle assessment of rice husk ash containing concrete. *Case Stud. Constr. Mater.* 2025, 23:e05241

[24] Habibi A, Ramezanianpour AM, Mahdikhani M, Bamshad O. RSM-based evaluation of mechanical and durability properties of recycled aggregate concrete containing GGBFS and silica fume. *Constr. Build. Mater.* 2021, 270:121431.

[25] Rasheed S, Hashmi I, Zhou Q, Kim JK, Campos LC. Central composite rotatable design for optimization of trihalomethane extraction and detection through gas chromatography: a case study. *Int. J. Environ. Sci. Technol.* 2023, 20(2):1185–1198.

[26] Patil SM, Malagi RR, Desavale RG, Sawant SH. Fault identification in a nonlinear rotating system using Dimensional Analysis (DA) and central composite rotatable design (CCRD). *Measurement* 2022, 200:111610.

[27] Nagaraju TV, Mantena S, Azab M, Alisha SS, El Hachem C, *et al.* Prediction of high strength ternary blended concrete containing different silica proportions using machine learning approaches. *Results Eng.* 2023, 17:100973.

[28] Zheng Y, Huang W, Du Z, Qiao L, Qu B, *et al.* Durability for solidified body of desulfurization wastewater from coal-fired power plants (In Chinese). *Clean Coal Techno.* 2022, 28(5):204–210.

[29] Tang J, Cao J, Luo H, Chen W, Jia Z, *et al.* The effect of demolition concrete waste on the physical, mechanical, and durability characteristics of concrete. *Buildings* 2024, 14(4):1148.

[30] Barker GC, Mehta A. Vibrated powders: structure, correlations, and dynamics. *Phys. Rev. A* 1992, 45(6):3435–3446

[31] Scrivener KL, John VM, Gartner EM. Eco-efficient cements: potential economically viable solutions for a low-CO2 cement-based materials industry. *Cem. Concr. Res.* 2018, 114:2–26.

[32] Cho BH, Chung W, Nam BH. Molecular dynamics simulation of calcium-silicate-hydrate for nano-engineered cement composites—a review. *Nanomaterials* 2020, 10(11):2158.

[33] Duque-Redondo E, Masoero E, Manzano H. Nanoscale shear cohesion between cement hydrates: the role of water diffusivity under structural and electrostatic confinement. *Cem. Concr. Res.* 2022, 154:106716.